Efficient Derivation of Lateral Plate and Paraxial Mesoderm Subtypes from Human Embryonic Stem Cells Through GSKi-Mediated Differentiation

Jia Yong Tan,[1] Gopu Sriram,[1] Abdul Jalil Rufaihah,[2] Koon Gee Neoh,[3] and Tong Cao[1]

The vertebrae mesoderm is a source of cells that forms a variety of tissues, including the heart, vasculature, and blood. Consequently, the derivation of various mesoderm-specific cell types from human embryonic stem cells (hESCs) has attracted the interest of many investigators owing to their therapeutic potential in clinical applications. However, the need for efficient and reliable methods of differentiation into mesoderm lineage cell types remains a significant challenge. Here, we demonstrated that inhibition of glycogen synthase kinase-3 (GSK-3) is an essential first step toward efficient generation of the mesoderm. Under chemically defined conditions without additional growth factors/cytokines, short-term GSK inhibitor (GSKi) treatment effectively drives differentiation of hESCs into the primitive streak (PS), which can potentially commit toward the mesoderm when further supplemented with bone morphogenetic protein 4. Further analysis confirmed that the PS-like cells derived from GSKi treatment are bipotential, being able to specify toward the endoderm as well. Our findings suggest that the bipotential, PS/mesendoderm-like cell population exists only at the initial stages of GSK-3 inhibition, whereas long-term inhibition results in an endodermal fate. Lastly, we demonstrated that our differentiation approach could efficiently generate lateral plate ($CD34^+KDR^+$) and paraxial ($CD34^-PDGFR\alpha^+$) mesoderm subsets that can be further differentiated along the endothelial and smooth muscle lineages, respectively. In conclusion, our study presents a unique approach for generating early mesoderm progenitors in a chemically directed fashion through the use of small-molecule GSK-3 inhibitor, which may be useful for future applications in regenerative medicine.

Introduction

EMBRYONIC STEM CELLS (ESCs) are endowed with the potential of indefinite self-renewal and the capacity to differentiate into all cell types of the three germ layers [1]. Due to these unique properties, therapeutic applications based on ESCs, an unlimited, renewable source of cells have become an attractive concept in regenerative medicine [2]. The development of ESC-based therapies necessitates an in-depth understanding of the complex signaling pathways involved during the differentiation process. To this end, numerous growth factors/cytokine combinations are currently being evaluated in order to understand the molecular mechanisms governing lineage commitment of ESCs and to establish differentiation protocols that drives their differentiation toward specific cell types.

The derivation of mesoderm lineage cell types, in particular, those with vascular [3–5] and hematopoietic potential [6,7], has been a focus of many investigators in the field of

ESC research. The interest in the generation of these cells stems from their therapeutic potential in the treatment of cardiovascular diseases and applications in tissue engineering [8,9]. Certain cell types are region specific. For example, the skeletal musculature arises from the paraxial mesoderm [10], while cardiac progenitors have been reported to be derived from the lateral plate mesoderm [11]. As such, efficient derivation of these cells may also require efficient differentiation toward their specific mesoderm subtypes. The vascular endothelial growth factor receptor 2 (*VEGFR2* or *KDR*) and platelet-derived growth factor receptor-alpha (*PDGFRα*) have been identified as useful surface markers that distinguish the lateral plate and paraxial mesoderm [12,13]. Despite the enormous progresses made in differentiating ESCs into these functional cell types, the need for efficient, time- and cost-effective methods of differentiation to reliably commit and expand therapeutically relevant and lineage-specific cells remains a major challenge before ESC-based therapies becomes a clinical reality.

[1]Oral Sciences, Faculty of Dentistry, National University of Singapore, Singapore, Singapore.
[2]Department of Surgery, Yong Loo Lin School of Medicine, National University of Singapore, Singapore, Singapore.
[3]Department of Chemical and Biomolecular Engineering, National University of Singapore, Singapore, Singapore.

During gastrulation, a specific subset of epiblast cells ingresses into the primitive streak (PS) from which the mesoderm emerges within the posterior region [14]. Since the formation of PS marks the initial specification step that generates all mesodermal and endodermal tissue lineages during early embryogenesis, efficient differentiation toward the PS would be an important first step toward increasing mesoderm yield during in vitro ESC differentiation. The canonical Wnt pathway is among the several identified signaling pathways playing a crucial role the gastrulation process. Genetic studies in mice have shown that embryos deficient in the canonical ligands of Wnt3 and its co-receptors, Lrp5/6 or lacking the downstream effector, β-catenin, are unable to establish the PS and eventually failed to generate the mesoderm [15–18]. These findings, along with recent reports on the in vitro differentiation of mouse ESCs (mESCs), demonstrated the requirement for Wnt/β-catenin activity in germ layer specification [19–21], although studies have also implicated its role in the maintenance of mESCs [22–24]. Instead, the role of Wnt/β-catenin signaling in human ESCs (hESCs) has been more controversial due to contradictory results among recent studies. Activation of the Wnt pathway using Wnt3a or BIO, an inhibitor of glycogen synthase kinase-3 (GSK-3), was observed to maintain hESCs in its undifferentiated state [25,26]. Other reports, however, demonstrated differentiation toward the PS and definitive endoderm lineages under the influence of Wnt signaling [27–29]. Thus, whether Wnt/β-catenin maintains hESCs in its undifferentiated state, or whether it promotes differentiation remains a subject of debate.

While there are multiple studies demonstrating mesodermal differentiation of hESCs, attention has largely been focused on the derivation of mature mesoderm cell types instead of the early events of germ layer specification, which could play a significant role in the effectiveness of the differentiation approach. In this work, we aimed at demonstrating efficient differentiation of hESCs into the mesoderm by inducing PS formation as an initial differentiation step and at identifying the earliest time point at which the two distinct mesoderm subtypes can be derived. We report that short-term activation of the Wnt/β-catenin pathway through the inactivation of GSK-3 using small-molecule inhibitors is sufficient to induce differentiation into a PS-like population, while long-term inactivation of GSK-3 results in an endodermal fate. The PS-like cells derived from GSK inhibitor (GSKi) treatment are demonstrated to be bipotential, being able to commit toward both the endoderm and mesoderm fate. Based on our findings, we further established a simple, yet efficient protocol by which hESCs can be differentiated into $CD34^+KDR^+$ and $CD34^-PDGFR\alpha^+$ mesoderm subsets from which we demonstrated further specification toward vascular endothelial and smooth muscle lineages, respectively. Access to these mesoderm derivatives in an efficient and time-effective approach could present opportunities for cell-based therapeutic strategies while bridging the gap between translational research and clinical applications.

Materials and Methods

hESC feeder-free culture

H1 and H9 hESC lines were purchased from Wicell Research Institute (Madison, WI) and maintained on Matrigel-coated six-well tissue culture plates in complete mTeSR™1 medium (STEMCELL Technologies). Both cell lines were routinely characterized and found to have expression of pluripotency markers *OCT4*, *SSEA4*, and alkaline phosphatase (Supplementary Fig. S1; Supplementary Data are available online at www.liebertpub.com/scd). Every 5–7 days, cells were passaged by exposure to 1 mg/mL dispase (Invitrogen) for 5–10 min at 37°C. hESC colonies were then harvested, dissociated into small clumps by gentle vortexing, and re-plated onto Matrigel-coated six-well plates at five colonies per well.

Differentiation of hESCs

All differentiation studies were carried out under feeder-free, chemically defined conditions. To study the effect of GSK inhibition on the fate of hESCs, the colonies were first dissociated into small clumps and re-plated onto Matrigel-coated six-well plates as per normal routine passaging. After 48 h, mTeSR medium was replaced with basal differentiation media (STEMdiff APEL; STEMCELL Technologies) supplemented with 5 μM GSKi (CHIR99021; Stemgent) for 5 days. For endoderm and mesoderm differentiation, the hESCs were first differentiated in the presence of 5 μM GSKi for 24 h, and further differentiated in basal differentiation media supplemented with either 25 ng/mL human recombinant Activin A (R&D Systems) or in 25 ng/mL rh-bone morphogenetic protein 4 (rhBMP4; Peprotech). Mesoderm differentiation was conducted in parallel with continuous GSKi treatment to compare the transcription profiles of endoderm- and mesoderm-associated genes. Concurrently, a separate group was also differentiated in BMP4 without prior GSKi treatment. When applicable, 10 μM SB431542 (Sigma) was added along with BMP4 during mesoderm specification or with Activin A during endoderm differentiation.

To induce further differentiation toward the vascular endothelial and smooth muscle lineages, GSKi-treated hESCs were differentiated in the presence of 25 ng/mL rhBMP4 for 24 h and further treated with basal differentiation media supplemented with 50 ng/mL VEGF (Peprotech) and 25 ng/mL rhBMP4 for 2 days. $CD34^+KDR^+$ and $CD34^-PDGFR\alpha^+$ subpopulations were sorted using fluorescence-activated cell sorting (FACS; Dako Cytomation MoFlo cell sorter) and seeded onto collagen IV-coated plates. The post-sorted $CD34^+KDR^+$ cells were further committed toward the endothelial lineage in ECGM-MV2 (Promocell) endothelial media supplemented with 50 ng/mL VEGF, and the $CD34^-PDGFR\alpha^+$ subpopulation was cultured in SMCGM2 (Promocell) smooth muscle media supplemented with 50 ng/mL $PDGF_{bb}$ (Molecular Probes) to induce smooth muscle lineage. After three passages, cells were harvested and compared with human umbilical vein endothelial cells (HUVECs) and human coronary artery smooth muscle cells (hCA-SMCs; Lonza) for gene expression levels of *CD31*, *vWF*, *VE-cadherin*, *α-SMA*, *SM22α*, and *PDGFRβ*.

Acetylated-low-density lipoprotein uptake assay

Low-density lipoprotein (LDL) uptake assay was performed by incubating the hESC-derived ECs with 10 μg/mL of Dil-Acetylated-LDL (Invitrogen) for 4 h. After washing twice with phosphate buffered saline (PBS), the nuclei were counterstained with Hoechst 33258 (Sigma). LDL uptake was viewed under an Olympus IX70 fluorescence microscope.

Matrigel tube formation assay

Tube formation assay was done according to the published work of Vo et al. [30]. Briefly, 10 μL of Matrigel (BD Bioscience) was pipetted into each well of a μ-Slide Angiogenesis (iBidi) and allowed to undergo gelation at 37°C for 1 h. To assess the ability of hESC-derived ECs to form vascular tube-like structures, 1×10^4 hESC-ECs were seeded onto each well of Matrigel-coated ibidi slides and incubated at 37°C for 18 h. Formation of vascular tube-like structures was observed under a phase-contrast microscope (Olympus IX70).

Flow cytometry

Differentiated cells were dissociated into a single-cell suspension using accutase (STEMCELL Technologies) and resuspended in PBS with 0.5% bovine serum albumin (BSA). To block non-specific binding of antibodies, cells were blocked with FcR blocking agent (1:10; Miltenyi Biotec) and incubated for 10 min at 4°C–8°C. For labeling of cell surface antigens, the cells were incubated with the following antibodies for 20 min at 4°C–8°C: *KDR*-phycoerythrin (PE), *PDGFRα*-fluorescein isothiocyanate (FITC), *VE-Cadherin*-allophycocyanin (APC) (all from R&D Systems), *KDR*-APC, *CD34*-APC or *CD34*-FITC, *CD31*-FITC (all from Miltenyi Biotec), and *CXCR4*-PE (BD Biosciences). For intracellular labeling of *SOX17*-Alexa Flour 488 (BD Biosciences), *Calponin*, and *α-SMA*, the procedure was performed using BD cytoperm/cytofix™ as per manufacturer's instructions. Indirect labeling of intracellular antigens *Calponin* and *α-SMA* was done using goat anti-mouse Alexa Flour 488 as secondary antibody. After incubation of antibodies, cells were washed thrice with PBS (0.5% BSA) to remove unbound antibodies. Flow cytometric data were collected using a Dako Cytomation CyAn ADP cytometer and analyzed with FlowJo Version 7.6.5 (TreeStar).

Quantitative real-time polymerase chain reaction

Total RNA was isolated from the cells using RNeasy Mini plus Kit (Qiagen) and reverse transcribed using iScript™ cDNA synthesis Kit (Biorad) at 500 ng total RNA per sample according to the manufacturer's protocol. All real-time polymerase chain reaction (RT-PCR) experiments were performed in triplicates using ABI StepOnePlus Real-Time PCR System and Fast SYBR-Green Master Mix as per the manufacturer's instructions (Applied Biosystems). The thermal cycling conditions included an initial denaturation step at 95°C for 10 min, 40 cycles at 95°C for 15 s, and 60°C for 1 min. The data are presented as fold changes in target gene expression calculated using the $2^{-\Delta\Delta CT}$ method normalized to the internal control gene (β-actin) and relative to control samples (day 0, undifferentiated hESCs). Details of primer sequences used for quantitative RT-PCR (qRT-PCR) are described in Supplementary Table S1. Results are presented as mean ± s.e.m. of three independent experiments unless otherwise stated.

Immunoflourescence

For immunofluorescence analysis, cells were fixed with 4% paraformaldehyde for 15 min and permeabilized with 0.2% Triton X-100 for 20 min. To block non-specific staining, cells were incubated with 5% goat serum/PBS for 1 h at room temperature. Subsequently, the cells were incubated with primary antibodies overnight at 4°C, followed by incubation with secondary antibodies, and counterstained with 4′,6-diamidino-2-phenylindole (DAPI). Alexa Fluor 488- and 596-conjugated secondary antibodies were purchased from Molecular Probes. Primary antibodies against the following proteins were used: mouse monoclonal *OCT4* (Santa Cruz), rabbit polyclonal *Brachyury*, rabbit polyclonal *beta-Catenin* (both from Abcam), mouse monoclonal *CD31*, mouse monoclonal *VE-Cadherin*, mouse monoclonal *α-SMA* (all from R&D Systems), mouse monoclonal *Calponin*, and rabbit polyclonal *vWF* (Abcam). Antibodies used for immunofluorescence and flow cytometry are shown in Supplementary Table S2.

Results

Despite the growing body of literature, the role of Wnt/β-catenin signaling in hESCs has remained controversial due to conflicting reports demonstrating either stem cell differentiation or self renewal. In this study, we activated the Wnt/β-catenin pathway using a selective inhibitor of GSK-3 and investigated its effects on the fate of hESCs. The transcriptional profiles of genes associated with both pluripotency and early differentiation were first analyzed using RT-qPCR.

Inhibition of GSK-3 under feeder-free, chemically defined conditions up-regulate PS-associated genes in hESCs in as early as 24 h

Profound changes in gene expression were detected during the time course of GSKi treatment (Fig. 1A). Pluripotency markers *SOX2* and *NANOG* were down-regulated, while *OCT4* appears to be maintained at 24 h of differentiation. The transient PS and early mesoderm population is characterized by expression of *MIXL1* and *T* (*Brachyury*) [31,32], although genes characteristic of early definitive endoderm such as *FOXA2* and *Goosecoid* (*GSC*) [33,34] are also expressed. Compared with hESCs treated in basal differentiation media alone, the addition of GSKi (CHIR99021) significantly elevated the transcript levels of *T* in just 24 h. The transcription profiles of both *T* and *OCT4* are comparable, with both reaching a peak at day 1 and down-regulated progressively thereafter. Similarly, *MIXL1*, as well as *FOXA2* and *GSC*, both of which are expressed in the anterior PS, were observed to follow a similar trend. Based on titration analysis, the up-regulation of *T* at day 1 is only possible with a concentration of 5 μM CHIR99021 and above (Supplementary Fig. S2A). Immunofluorescence analysis confirmed the up-regulation of *T* and the presence of *OCT4* after 24 h of GSKi treatment in both H1 and H9 hESC lines (Fig. 1B for H1 and Supplementary Fig. S2C for H9). As cells began moving out from the periphery of the colony at day 2, both *T* and *OCT4* were visibly down-regulated. Differentiation in basal media alone is insufficient to induce *T* expression (Supplementary Fig. S2C). Further, GSKi-treated colonies showed signs of nuclear accumulation of *β*-catenin as they appeared to be spread throughout individual cells; whereas they were more localized at the cell periphery in hESCs and no-GSKi control groups (Fig. 1C and 20× magnification in Supplementary Fig. S2D). These observations established the involvement of GSKi in the transient up-regulation of *T* and suggest the existence of a "temporal window" during the early stages of differentiation
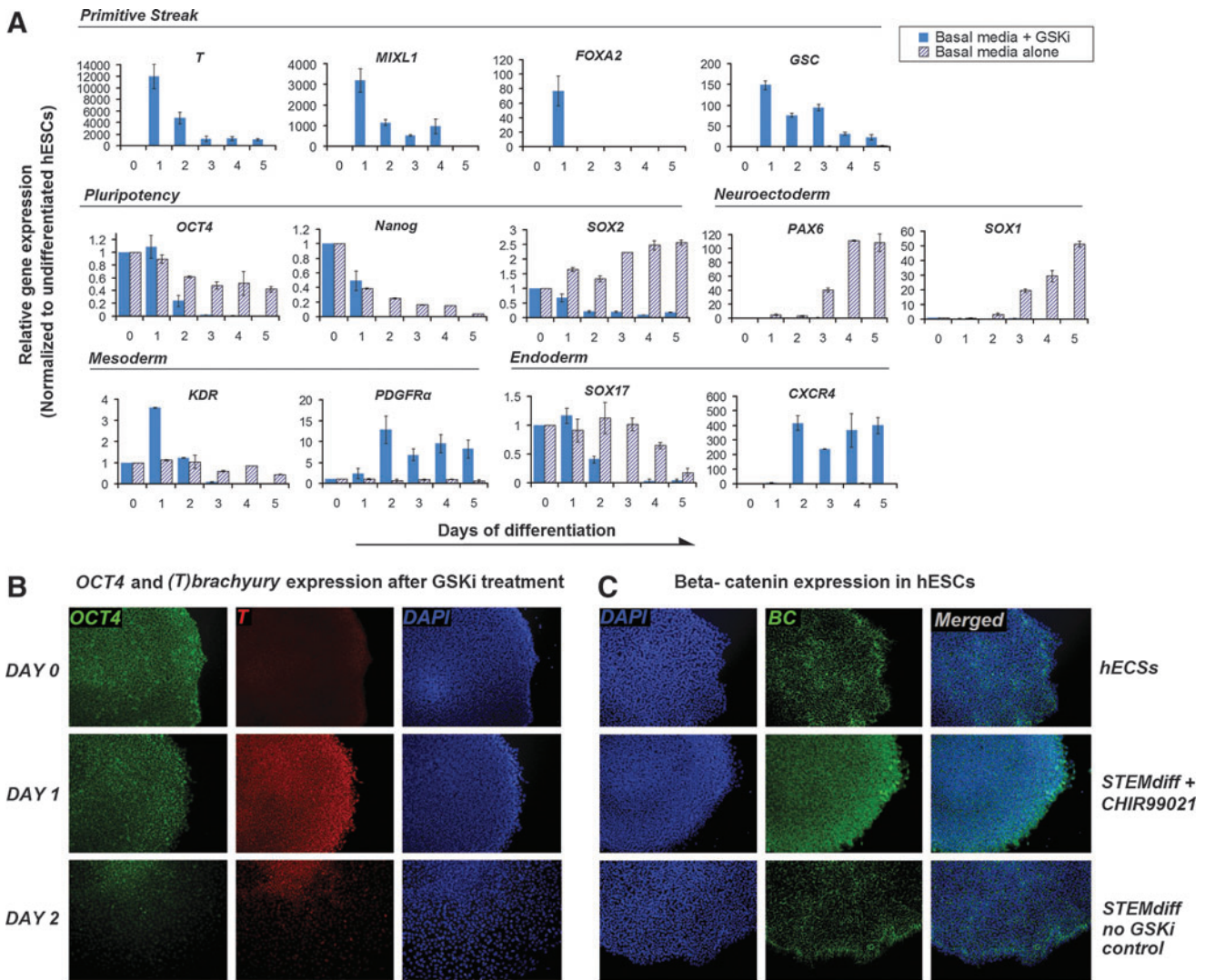
FIG. 1. Time-course analysis of the transcriptional profiles of genes associated with both pluripotency and early differentiation in GSKi-treated hESCs. **(A)** H1-hESCs were treated with 5 μM CHIR99021 using STEMdiff APEL as the basal differentiation media without additional growth factors/cytokines under feeder- and serum-free conditions. Subsequently, RNA was extracted from GSKi-treated hESCs at 24 h intervals from day 0 to 5, and quantitative real-time PCR (qRT-PCR) analysis was performed using primers specific to PS (*T*, *MIXL1*, *GSC*, and *FOXA2*), pluripotency (*OCT4*, *NANOG*, and *SOX2*), mesoderm (*KDR* and *PDGFRα*), ectoderm (*SOX1* and *PAX6*), and endoderm (*CXCR4* and *SOX17*) genes. The transcript levels of PS-associated genes were up-regulated in just 24 h of GSKi treatment and were subsequently down-regulated thereafter. All qRT-PCR data were normalized to β-actin as an endogenous control and were presented as expression levels (fold) relative to day 0, with undifferentiated hESCs as controls. **(B)** *T (brachyury)* and *OCT4* expression was analyzed by immunofluorescence microscopy. *T* was visibly detected in hESCs after 24 h of GSKi treatment and began to down-regulate by day 2. **(C)** *β-catenin* expression in hESCs after GSKi treatment. *Top row*: *β-catenin* expression in undifferentiated hESCs, *middle row*: after 24 h of GSKi treatment, *bottom row*: no-GSKi control. All scale bars represent 200 μm. GSK, glycogen synthase kinase; GSKi, GSK inhibitor; hESCs, human embryonic stem cells; PS, primitive streak; *GSC*, *Goosecoid*. Color images available online at www.liebertpub.com/scd

where the expression of pluripotency and PS markers may overlap.

We further analyzed the expression of endoderm, ectoderm, and mesoderm associated genes in GSKi-treated hESCs. In the absence of GSKi, the up-regulation of *SOX1* and *PAX6* beginning at day 3 indicates presumptive neuroectoderm induction. Otherwise, the expression levels of these two markers appear to be down-regulated throughout the entire time course, which suggest a non-ectodermal route of differentiation under GSKi treatment. Endoderm marker *SOX17* remained at low levels with no noticeable up-

regulation, while *CXCR4* was markedly increased starting only at day 2. Following the trend of PS markers, the lateral plate mesoderm marker *KDR* was transiently up-regulated after 24 h of exposure to GSKi. Coincidentally, its down-regulation beginning at day 2 was met with the elevated expression of paraxial mesoderm marker *PDGFRα* on the same day, suggesting that prolonged GSKi treatment may favor differentiation toward the paraxial mesoderm fate. Using a different GSKi, CHIR98014 (Selleckchem), a similar transcription profile was observed for *CXCR4* and *T* with significant up-regulation occurring at days 2 and 1,

respectively (Supplementary Fig. S2B). Similar to CHIR99021, *T* expression and the nuclear accumulation of *β*-catenin can be induced by CHIR98014 (Supplementary Fig. S2C and S2D, respectively). Taken together, our findings propose that GSKi treatment is unable to maintain the pluripotent status of hESCs but triggers differentiation to a state resembling the PS in as early as 24 h based on an analysis of the transcription profiles of PS-associated genes.

A PS/mesendoderm-like population exists in the early stages of GSK-3 inhibition, whereas prolonged inhibition results in a pure CXCR4⁺ population
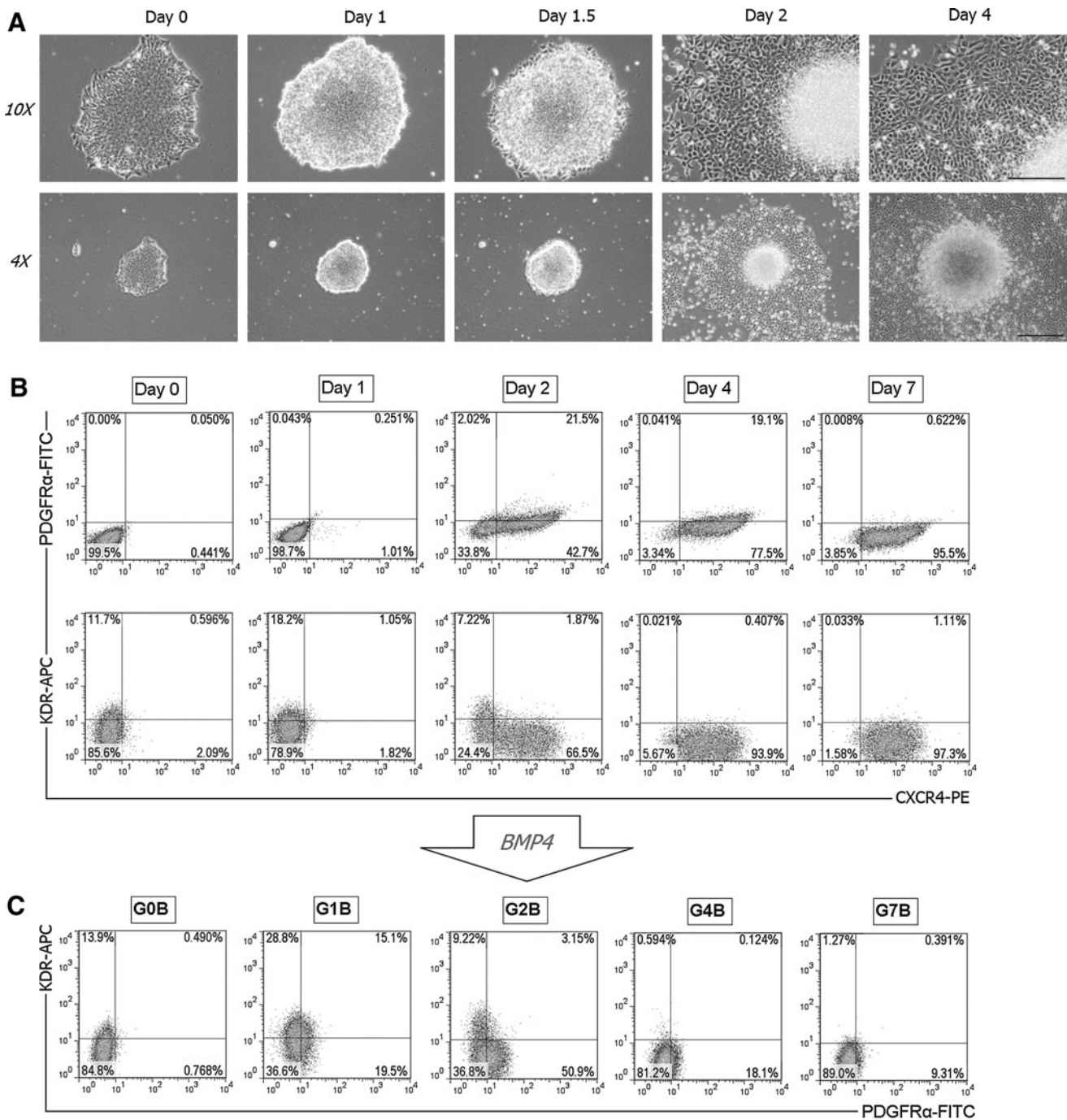
Our analysis on the transcription profiles of PS-associated genes in Fig. 1 suggests that the GSKi-treated hESCs at day 1 may be a source of cells representing the mesendoderm. At this time point, the hESC colonies appear to have shrunk slightly, with the edges of the colony starting to pull away from the plate (Fig. 2A). Prolonged GSKi treatment for more than 24 h resulted in morphological changes that are characterized by small, cobblestone-like cells spreading outward from the edges of the colony. We note that this outgrowth of cells seems to coincide with the transcription profile of *CXCR4*, which is up-regulated starting at day 2. These observations are in line with our time-course FACS analysis that detected the large emerging population of $CXCR4^+$ cells after 2 days of GSKi treatment (Fig. 2B). In basal media alone, $CXCR4^+$ cells remained undetected (Supplementary Fig. S3A). On the same day, the mesoderm marker *PDGFRα* was also detected in some of the $CXCR4^+$ cells, although its expression decreased by day 4 and was undetectable at day 7. *KDR* was lowly expressed in its undifferentiated state, and the number of KDR^+ cells increased slightly after 24 h of exposure to GSKi. By day 4, the differentiated cells were almost entirely positive for *CXCR4* and negative for *KDR*, which indicates a purely endodermal fate under prolonged GSKi treatment. Despite the abundance of $CXCR4^+$ cells, *SOX17* was not detected throughout the course of GSKi treatment (data not shown).

We next investigated the mesoderm potential of the GSKi-treated hESCs. BMPs are multifunctional growth factors that comprise a subfamily of the transforming growth factor β (TGFβ) superfamily. Their roles in embryonic development and cellular functions in postnatal and adult animals have been extensively studied in recent years. Typically, BMP4 is known for inducing pluripotent stem cell (PSC) differentiation into both hematopoietic [35] and endothelial cells [36] as well as in trophoblast [37] and extra-embryonic endoderm [38]. In addition, BMP4 signaling is also critical for bone and cartilage formation, as it has been shown to promote chondrogenic and osteogenic differentiation in stem cells [39]. A recent study suggested its role as a mesoderm inducer during hESC differentiation [40]. Here, we administered BMP4 after hESCs had been treated with GSKi for varying durations and analyzed the expression of mesoderm markers *KDR* and *PDGFRα* after 24 h of exposure to BMP4. FACS analysis confirmed that BMP4 treatment promoted the development of both mesoderm subtypes in the group that underwent prior GSKi treatment for 1 day (G1B) (Fig. 2C). A small fraction of cells was observed to be double positive for *KDR* and *PDGFRα*, which was expected as both lateral and paraxial mesoderm populations emerge adjacent to each

other during embryogenesis with overlapping gene expression patterns. For the group that underwent 2 days of GSKi treatment before BMP4 culture (G2B), the number of cells expressing *KDR* decreased considerably while $PDGFRα^+$ cells increased after 24 h of exposure to BMP4. From the representative dot plot, the *KDR* and *PDGFRα* populations appears to be more distinct as compared with the G1B group. The expression of both markers, in particular, *PDGFRα* was noticeably decreased in the G4B group and was almost undetectable in the G7B group, indicating that exposure to BMP4 after prolonged GSKi treatment had failed to induce mesoderm differentiation. As the differentiated cells become fully committed toward the endoderm fate due to prolonged inactivation of GSK-3, the number of cells that could potentially differentiate toward the mesoderm decreases. These findings demonstrate that cells with mesoderm potential exist only at the initial stages of GSK inhibition, preferably within 2 days after exposure to GSKi. In the next section, we show that the GSKi-treated hESCs at this time point (the G1B group) are also bipotential, with the capability of differentiating toward the endoderm without prolonged GSKi treatment.

GSKi-treated hESCs have potential to commit toward the endoderm under Activin A treatment

Based on our findings pertaining to the use of GSKi, we sought to investigate the endoderm potential of GSKi-treated hESCs. Accordingly, the endodermal differentiation experiment was performed after initial GSKi treatment for 24 h in chemically defined, feeder-free conditions, without additional growth factors/cytokines other than the ones mentioned in this section. Among the growth factors tested, endoderm formation was most pronounced in the presence of exogenous Activin A, while exposure to BMP4 after GSKi treatment induced mesoderm lineage commitment (Fig. 3A, B). Exposure to Activin A for a period of 2 days resulted in significant up-regulation of endoderm markers *FOXA2*, *SOX17*, and *CXCR4* (Fig. 3B). In addition, the transcripts of mesoderm-associated genes *KDR* and *PDGFRα* remained at low levels during Activin A treatment but was markedly up-regulated in the group treated with BMP4 (Fig. 3B). Remarkably, exposure of GSKi-treated hESCs to Activin A alone yielded ∼75% of cells expressing *SOX17* and 52% $CXCR4^+$ cells, while the faction of cells expressing mesoderm markers *KDR* and *PDGFRα* remained negligible after 48 h (Figs. 3C and 4A). To further demonstrate the involvement of Activin/Nodal signaling in endoderm commitment, the differentiation media was simultaneously administered with SB431542, a selective inhibitor of the TGFβ type I activin receptor-like kinases (ALK), specifically ALK4, ALK5, and ALK7. Compared with the group treated with Activin A alone, gene expression analyses revealed the distinctively lower transcript level of *CXCR4* and the complete abolishment of *SOX17* and *FOXA2* with the addition of SB431542 (Fig. 3B). This endoderm-suppressing effect of SB431542 was further confirmed by FACS analysis, which detected little or no expression of *CXCR4* and *SOX17* (Fig. 3C). Interestingly, the combination of SB431542 and Activin A also increases the proportion of both $PDGFRα^+$ and KDR^+ cell population. This suggests that the GSKi-treated hESCs which were originally fated for endodermal differentiation during

FIG. 2. A PS/mesendoderm-like cell population exists in the initial stages of GSKi treatment as analyzed by FACS. **(A)** The representative morphology of the hESC colonies under GSKi treatment at the indicated time points was shown. Scale bars: 500 μm for 10× magnification (*top row*), 1 mm for 4×(*bottom row*). **(B)** Time-course FACS analysis in GSKi-treated hESCs. Cells were harvested at different time points (days 0, 1, 2, 4, and 7) and stained with *KDR*-APC, *PDGFRα*-FITC, and *CXCR4*-PE for FACS analysis. Cells expressing *CXCR4* were detected starting at day 2 of GSKi treatment, which is also concurrent with the morphological spreading of cells from the edges of the hESC colony. Prolonged inhibition of GSK-3 eventually resulted in a pure *CXCR4*$^+$ cell population. **(C)** Analysis on the mesoderm potential of hESCs after GSKi treatment. Cells were treated with BMP4 for 24 h after different durations of GSKi treatment as indicated: G1B, G2B, G4B, and G7B, the number representing the days of GSKi treatment. For the G0B group, hESCs were differentiated directly in BMP4 for 48 h without prior GSKi treatment. FACS, fluorescence-activated cell sorting; APC, allophycocyanin; FITC, fluorescein iso-thiocyanate; PE, phycoerythrin; BMP, bone morphogenetic protein.
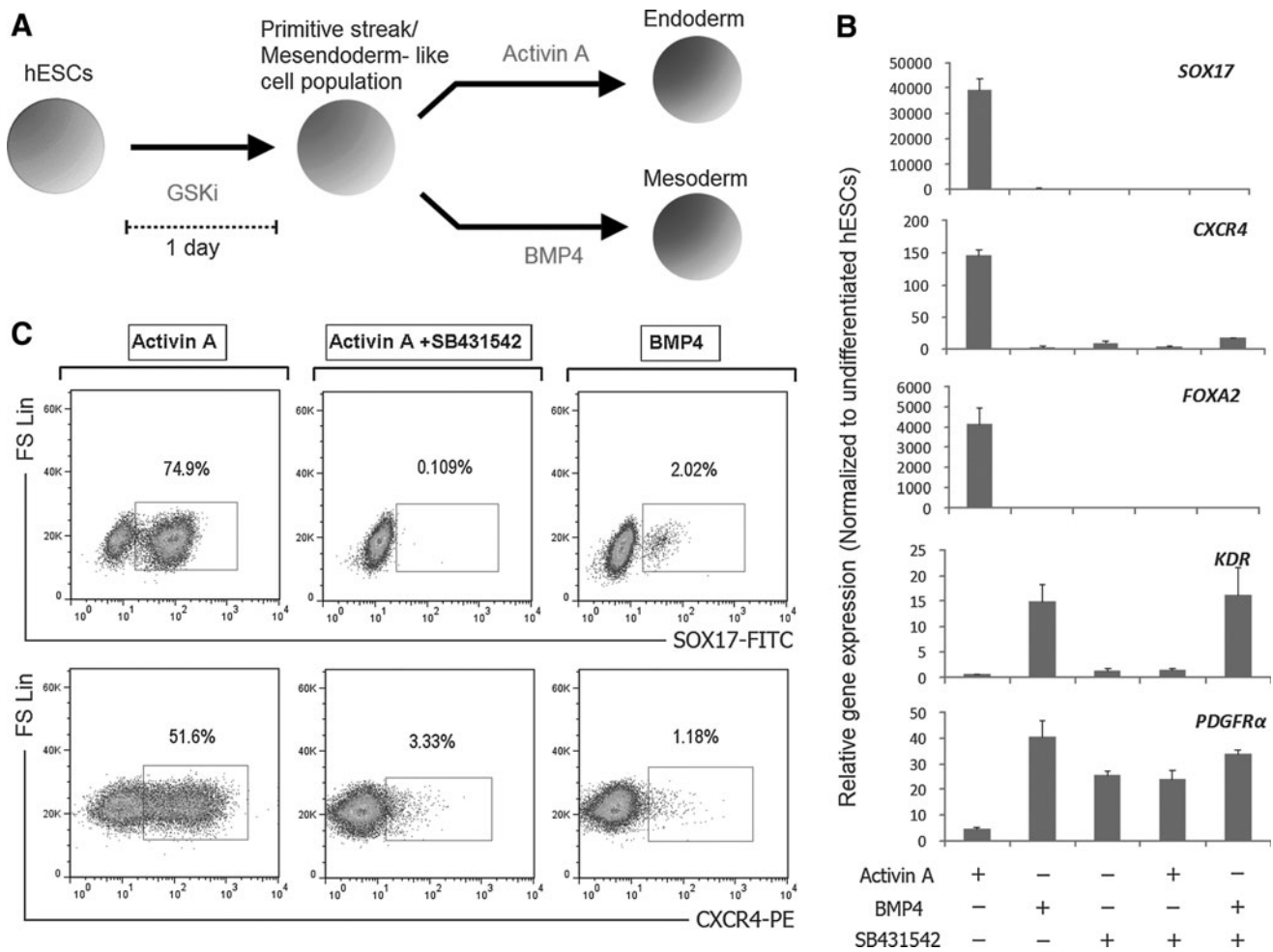
FIG. 3. hESCs treated with 5 μM GSKi for 24 h and subsequently in Activin A for 48 h differentiate toward the endoderm. **(A)** Illustration on the differentiation of hESCs based on the inhibition of GSK-3. hESCs were initially treated with 5 μM GSKi for 24 h to induce PS formation and further differentiated toward the endoderm using Activin A, or toward the mesoderm using BMP4. **(B)** GSKi-treated hESCs were further differentiated for 48 h in different growth factor combinations consisting of BMP4, Activin A, and SB431542. qPCR analysis was performed using primers specific to endoderm (*FOXA2*, *CXCR4*, and *SOX17*) and mesoderm (*KDR* and *PDGFRα*) genes. Activin A was shown to up-regulate endoderm-associated markers, while BMP4 up-regulated mesoderm markers. **(C)** Percentage of *CXCR4*⁺ and *SOX17*⁺ cells after 3 days of differentiation (initial 24 h in 5 μM GSKi, and 48 h in Activin A, Activin A + SB431542, or BMP4) as determined by flow cytometry. Activin A treatment alone resulted in a majority of cells expressing *CXCR4* and *SOX17*, but its endoderm-inducing effect was suppressed with the addition of SB431542.

Activin A treatment undergo mesoderm commitment under the effect of SB431542.

BMP4 treatment after initial exposure to GSKi drives hESC differentiation toward the mesoderm lineage and blocks endoderm differentiation

To further analyze the mesoderm potential of GSKi-treated hESCs, we administered BMP4 24 h after GSKi treatment and examined the transcription levels of *PDGFRα* and *KDR* at 24 h intervals. In contrast to hESCs that underwent continuous GSKi treatment, the gene expression of lateral plate marker *KDR* was significantly up-regulated after 24 h of exposure to BMP4 (Fig. 4B). Similarly, *PDGFRα* was up-regulated at day 2, although it decreased to levels comparable with continuous GSKi treatment by day 4. We, therefore, identified day 2 as the time point where the relevant mesoderm subsets were suffi-

ciently specified. Our FACS analysis also confirmed the mesoderm-inducing effect of BMP4 (Fig. 4A).

Next, we compared the gene expression of these markers in hESCs that were differentiated in BMP4 without prior GSKi treatment. In a way, this comparison allows us to determine whether the expression of these markers can be influenced by upstream protocols in mesoderm induction. From RT-qPCR analysis, the transcripts of PS/early mesoderm markers *T* and *MIXL1* were elevated in both groups, although it was distinctively higher in the group that had been initially differentiated with GSKi (Supplementary Fig. S3B). Following our protocol, *KDR* was noticeably up-regulated after 24 h in BMP4 to levels higher than the group that was differentiated directly in BMP4 without using GSKi from the onset. These data correspond well with our FACS analysis in Fig. 2C, where abrogation of the initial GSKi treatment step (the G0B group) resulted in a smaller fraction
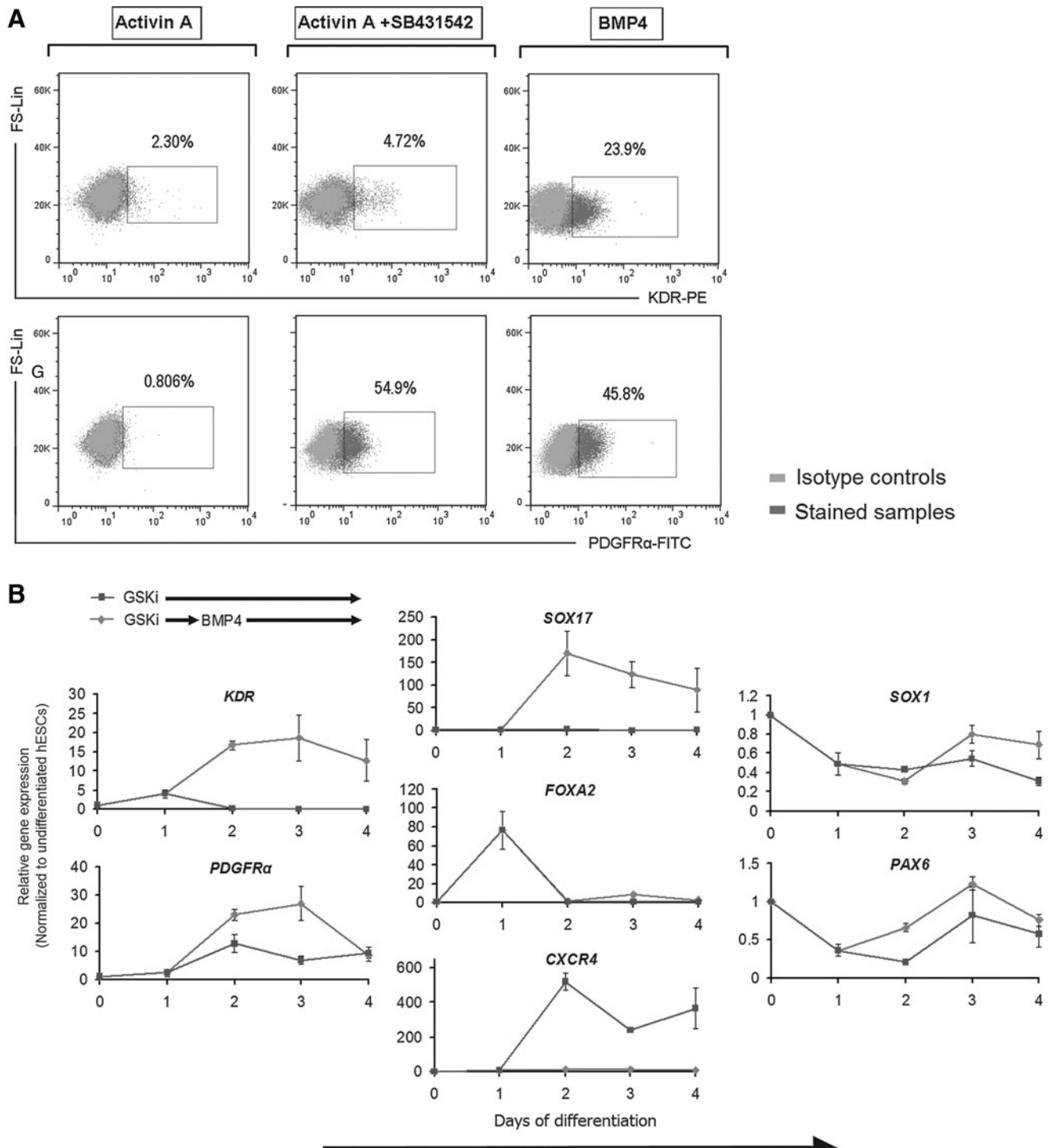
FIG. 4. BMP4 drives mesoderm differentiation of GSKi-treated hESCs. **(A)** Flow cytometric analysis of KDR^+ and $PDGFR\alpha^+$ cells demonstrating the mesoderm-inducing effect of BMP4 after 3 days of differentiation (24 h in GSKi and further 48 h in BMP4). Data presented are dot plots from stained samples (*dark gray*) overlaid with isotype controls (*light gray*). **(B)** hESCs were differentiated in 5 μM GSKi for 24 h and further differentiated in BMP4 for an additional 3 days (-◆-). The transcription levels of mesoderm, endoderm, and neuroectoderm-associated genes were compared with hESCs differentiated in GSKi for 4 days (-■-) using qRT-PCR. The transition to BMP4 culture from GSKi up-regulates mesoderm markers *KDR* and *PDGFRα* while suppressing *FOXA2* and *CXCR4*. All PCR data were normalized to β-actin expression and presented as relative expression (fold) using day 0 as control samples.

of KDR^+ cells, while cells expressing $PDGFR\alpha$ were not detected at all. This low yield may suggest that hESCs have yet to adopt a PS-like stage before specifying toward the mesoderm. This could also imply that activation of Wnt/β-catenin pathway using GSKi is a more effective approach to induce PS formation in hESCs than using BMP4, whose role, in our opinion, is more suited in transiting from the PS to the mesoderm.

In addition, we analyzed the expression of endoderm- and ectoderm-related genes in response to BMP4 treatment and found that most of these genes appear to be inhibited throughout the course of BMP4 treatment. $CXCR4$, which was noticeably up-regulated at day 2 under continuous GSKi treatment as shown in Fig. 1, was completely suppressed at all time points after switching to BMP4 culture (Fig. 4B). We also detected little or no expression of $FOXA2$, $PAX6$, and $SOX1$ throughout the course of differentiation. Interestingly, we found that, in the presence of BMP4, the gene expression of $SOX17$ was up-regulated within 24 h (day 2), although its transcript level was nowhere as high as the group treated under Activin A (see Figs. 3B and 4B). These observations correspond well with FACS data that detected minimal levels of $SOX17^+$ and $CXCR4^+$ cells in BMP4 cultures (Fig. 3C). Collectively, we showed that hESCs which underwent differentiation to the PS under the influence of GSKi (for 24 h) have the potential to further commit toward either the endoderm or mesoderm depending on the culture conditions. Along with our findings pertaining to the use of GSKi, we were able to establish a novel, stepwise mesoderm induction protocol for the directed differentiation of hESCs into the mesoderm lineage.

GSKi-derived mesoderm has the potential to further differentiate into endothelial and smooth muscle lineages

Among the three germ layers, the mesoderm is considered a potential source of progenitors giving rise to vascular endothelial cells and SMCs during embryonic development. A variety of markers have been used to identify progenitors that could give rise to ECs and SMCs, including $CD34$, $CD31$, KDR, and $PDGFR\alpha$ [4,41,42]. $CD34$ has generally been associated with progenitors for hematopoietic and endothelial lineages, whereas other studies have related $PDGFR\alpha$ with progenitors for cardiac, smooth muscle, and mesenchymal lineages. To further ascertain the potential of our GSKi-derived mesoderm, we further directed the differentiation of hESCs toward these two lineages. Differentiation was conducted in a stepwise approach that was similar to our mesoderm induction protocol but with an additional VEGF treatment step to induce vascular commitment (Fig. 5A). In just 24 h exposure to VEGF (day 3 of differentiation), the transcript levels for endothelial-associated markers such as $CD31$ and $CD34$ were visibly up-regulated (Fig. 5B). This follows after the increase in KDR and $PDGFR\alpha$ expression at day 2, which is in line with the down-regulation of T. Without VEGF, $CD34$ and $CD31$ remained down-regulated. Our time-course FACS analysis reveals that the $CD34^+$ cells starts moving out from the KDR^+ population at day 3 and amounts to approximately half of the entire cell population by day 4, of which most co-expressed $CD31$ (Fig. 5C). Almost all of the $CD34^+$ cells co-expressed KDR, but all were negative for $PDGFR\alpha$, which confirms their lateral plate

specificity (Fig. 5D). Similarly, the H9 hESC line showed comparable transcription profiles and also demonstrated efficient differentiation under the same protocol, although having a slightly lower percentage of cells expressing $CD34$, $PDGFR\alpha$, and KDR (Supplementary Fig. S4A, B). Likewise, the H1 cell line showed comparable differentiation efficiency using CHIR98014 as the GSKi.

From pre-sort analysis, both the $CD34^+KDR^+$ and $CD34^-PDGFR\alpha^+$ cell populations make up ∼51% and 35% of the total population, respectively (Supplementary Fig. S4D). After three passages in endothelial growth conditions, the post-sorted $CD34^+KDR^+$ cells displayed a flattened, cobblestone-like morphology and strongly expressed endothelial cell-specific proteins: $CD31$, vWF, and VE-$cadherin$ (Fig. 6A). The gene expression levels of these markers are comparable with HUVECs (Fig. 6B). The majority of the sorted $CD34^+KDR^+$ cells became $CD34^+CD31^+$ positive and remained negative for $PDGFR\alpha$, while KDR was down-regulated (Supplementary Fig. S4D). In addition, the cells were able to spontaneously reorganize into tube-like structures on Matrigel and were capable of acetylated-LDL uptake. FACS analyses also revealed that a majority of the pre-sorted $CD34^-$ cells express $PDGFR\alpha$, which indicates their paraxial mesoderm origin (Fig. 5D). In other reports, $CD34^-$ cells that are positive for $PDGFR\alpha$ have also been proposed to differentiate toward smooth muscle lineages [42]. After three passages in PDGF$_{bb}$-supplemented medium, the sorted $CD34^-PDGFR\alpha^+$ population expressed comparable levels of α-SMA, $SM22\alpha$, and $PDGFR\beta$ to hCA-SMCs with no detectable transcripts of endothelial markers (Fig. 6B). While $PDGFR\alpha$ expression is lost after a few passages, $CD31$ remained unexpressed, confirming their non-endothelial fate (Supplementary Fig. S4D). Further, immunoflourescence analysis corresponds with FACS data, which detected the presence of α-SMA and $calponin$ (Fig. 6A, C). These observations demonstrated the efficacy of our mesoderm induction approach in driving differentiation toward vascular endothelial and smooth muscle lineage under the right growth conditions.

Discussion

The development of successful ESC-based therapies requires an in-depth understanding of the complex signaling pathways governing lineage commitment and to establish robust, efficient, and reproducible protocols that direct their differentiation toward specific and therapeutically relevant cell types. To realize this potential, a plethora of differentiation methods to generate specific cell types have been devised. However, the rationale of the differentiation approach in a number of these existing protocols is often left unexplained, often involving spontaneous and/or one-step differentiation approaches in undefined conditions, and/or requires long-term culture that generates low yields with other undesirable cell types, rather than recapitulating the early events in germ-layer specification as a basis of their differentiation approach. Here, we presented a step-wise mesoderm induction method based on the use of small-molecule GSK-3 specific inhibitor and minimal growth factors, while elucidating the involvement of each factor at every step of the protocol. We believe that by recapitulating the early events of embryogenesis in culture, effective differentiation strategies can be formulated accordingly.
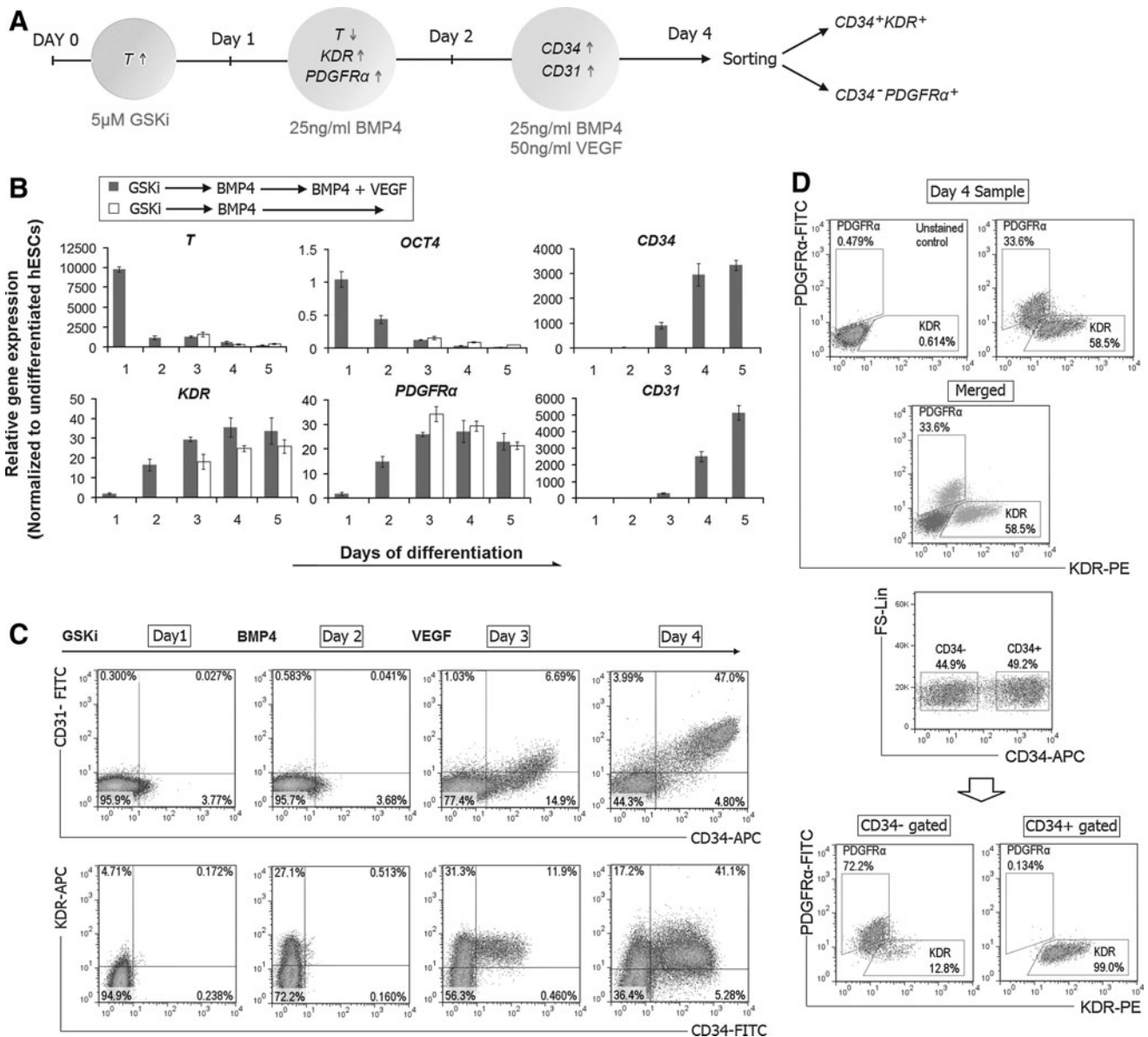
FIG. 5. Efficient and rapid differentiation of hESCs toward *CD34*$^+$ progenitors using a three-step differentiation procedure involving initial GSKi treatment. **(A)** Illustration of the protocol for hESC differentiation toward endothelial and smooth muscle lineage. After initial GSKi treatment for 24 h and further differentiation toward the mesoderm for an additional 24 h using BMP4, hESCs were further differentiated in VEGF-supplemented conditions. **(B)** Time-course qRT-PCR analysis on the entire differentiation process. As the mesoderm matures, *T* expression is down-regulated followed by the up-regulation of mesoderm markers (*KDR* and *PDGFRα*). The vascular inducing effect of VEGF is confirmed by the detection of *CD34* and *CD31* expression at day 3 of differentiation. **(C)** FACS analysis on the expression of the mesodermal markers *KDR*, *CD34*, and *CD31*. At day 3 of differentiation (after 24 h exposure to VEGF), *CD34*$^+$ cells were observed to emerge from the *KDR*$^+$ population (*left column*) and began to co-express *CD31* by day 4 (*right column*). **(D)** FACS analysis for day 4 samples stained with *KDR*-PE and *PDGFRα*-FITC. The representative dot plots of stained and unstained samples are overlaid, which revealed two distinct subpopulations representing *KDR*$^+$ and *PDGFRα*$^+$ cells (*upper panel*). *KDR* and *PDGFRα* expression in gated *CD34*$^+$ and *CD34*$^-$ subpopulations confirmed that all *CD34*$^+$ cells are negative for *PDGFRα* (*lower panel*). VEGF, vascular endothelial growth factor.

Inhibition of GSK-3 function leads to stabilization and translocation of *β-catenin* to the nucleus, where it associates with transcription factors of the T-cell factor (*TCF*) and lymphoid enhancing factor (*LEF*) families [43]. In this article, we demonstrated that short-term inhibition of GSK-3 efficiently induced differentiation of hESCs toward a PS/mesendoderm-like state, and that initial GSKi treatment followed by BMP4

supplementation efficiently drives differentiation of hESCs toward the mesoderm lineage. The concomitant peaking of *brachyury* expression and other PS-related genes in as early as 24 h in response to GSKi and their subsequent down-regulation is reminiscent of the transient nature of the PS during early embryogenesis. It was also interesting to note that the down-regulation of these genes at day 2 begins in tandem with the
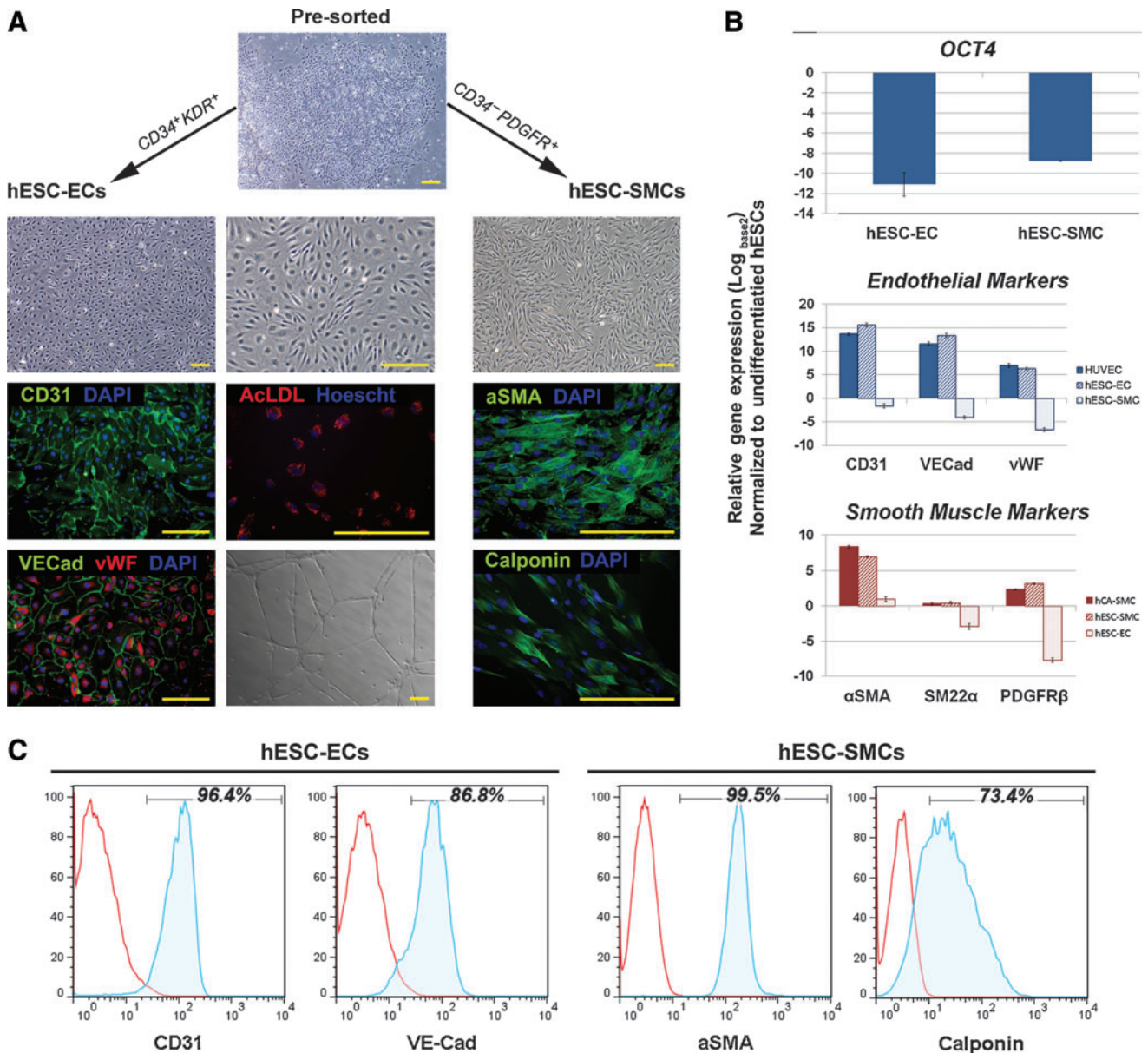
FIG. 6. The post-sorted $CD34^+KDR^+$ and $CD34^-PDGFR\alpha^+$ subpopulations demonstrated endothelial and smooth muscle potential, respectively. **(A)** Phase-contrast image represents the morphology of pre-sorted cells after 4 days of differentiation (*top*). Post-sorted $CD34^+KDR^+$ cells adopted an endothelial-like morphology in endothelial growth conditions and were stained positive for *CD31*, *vWF*, and *VE-cadherin* (*left column*). They were also capable of forming tube-like structures on Matrigel and demonstrated acetylated-LDL uptake (*middle column*). In smooth muscle growth conditions, the post-sorted $CD34^-PDGFR\alpha^+$ cells began to take on a spindle-shaped morphology and were positively stained for *α-SMA* and *calponin* (*right column*). Nuclei were counterstained with DAPI. All scale bars represent 200 μm. **(B)** hESC-derived endothelial and smooth muscle cells were harvested after three passages from sorting and analyzed for endothelial- and smooth muscle-associated gene expression (*CD34*, *CD31*, *vWF*, *VE-cadherin*, *α-SMA*, *PDGFRβ*, and *SM-MHC*) by RT-PCR. Relative gene expression levels were compared with umbilical vein endothelial cells (HUVECs) and human coronary artery smooth muscle cells (hCA-SMCs) relative to undifferentiated hESC controls. **(C)** Expression of *CD31*, *VE-cadherin*, *α-SMA*, and *calponin* in our hESC-derived endothelial and smooth muscle cells was further confirmed by FACS analysis. LDL, low density lipoprotein. Color images available online at www.liebertpub.com/scd

morphological spreading of cells from the edges of the hESC colony and the emergence of cells expressing *CXCR4*. While differentiation toward an endodermal fate via long-term inactivation of GSK-3 has been demonstrated, the short-term effects of GSKi treatment were not previously reported. Here, we showed that hESCs treated with GSKi for 24 h is sufficient to induce a mesendoderm-like cell population that is capable of

differentiation toward the endoderm or mesoderm. The rapid induction of the mesendoderm in this work may very well depict the events described in the study of Kemler et al. [44], where β-catenin stabilization in mutant mouse embryos leads to premature epithelial-mesenchymal transition and, thus, may be a point to be considered for differentiation protocols where time effectiveness is an issue.

A possible explanation to account for the controversies surrounding the role of Wnt/β-catenin signaling in hESCs is the presence of additional factors in the differentiated media used in various studies that could have interfered with Wnt signaling and/or activated other pathways. In one study that used mouse embryonic fibroblasts (MEF)-conditioned media, hESCs were observed as maintaining their undifferentiated morphology and proliferated when supplemented with Wnt3a [45]. One may argue that the presence of anti-differentiation factors, for example, basic fibroblast growth factor (bFGF) in conditioned media supports the maintenance of hESCs while under the influence of Wnt signaling. Supporting this hypothesis are studies showing the differentiation of hESCs under active Wnt signaling in the absence of bFGF but self renewal in the presence of exogenous bFGF [46,47]. This was, however, contradicted in another report demonstrating differentiation toward the endoderm lineage using mTeSR1 as the basal differentiation media, which is known to contain high concentrations of bFGF and other factors [28]. In our study, we showed that activation of the Wnt/β-catenin pathway using GSKi alone in feeder-free, chemically defined culture conditions without additional growth factors/cytokines drove hESC differentiation toward the PS.

During maturation of the mesoderm, *brachyury* expression is down-regulated and cells begin expressing *KDR* and *PDGFRα*. In the context of mesodermal differentiation, others have reported that initial BMP4 treatment was sufficient to drive hESC differentiation toward the mesoderm lineage [40,48]. In our experience, however, exposure to BMP4 without prior GSKi treatment was permissive, but not effective in mesoderm induction and it also failed to generate the paraxial subtype. Conversely, our findings pertaining to the use of BMP4 demonstrated efficient derivation of both the paraxial and lateral plate mesoderm subtypes in GSKi-mediated differentiation. These observations may be attributed to the addition of the GSKi treatment step, which effectively drove differentiation toward the PS, an essential specification step that generates all mesodermal tissues during the early developmental process. Further, the differences in culture conditions, with hESCs being cultured in MEF-conditioned medium before differentiation in these studies, may also explain the discrepancy in the use of BMP4 in our study. In support of this possible explanation, a study has shown that hESCs cultured under MEF-conditioned media displayed elevated expression of PS genes as compared with hESCs cultured in N2B27 medium, which indicates a pre-PS-like intermediate stage but still adopts an undifferentiated status [49]. Apparently, their differentiation in conditioned media is prevented because of factors present in knockout™ serum that stimulates phosphatidylinositol 3-kinase activity [50]. This may explain the ineffectiveness of using BMP4 as the initial differentiation step to drive PS/mesodermal differentiation in our study, as our hESCs are continuously passaged and cultured in mTeSR1 under feeder-free conditions, thus lacking these factors that would have "conditioned" the hESCs into a pre-PS-like stage. In this study, we were also able to demonstrate endodermal differentiation using Activin A alone in feeder-free, chemically defined conditions, which affirms the bipotential status of our GSKi-treated hESCs.

Collectively, we have established a novel, stepwise mesodermal differentiation approach by exploiting the use of

small-molecule inhibitors that are specific to GSK-3. Further differentiation toward the endoderm or mesoderm fate can be modulated by Activin/Nodal and BMP signaling pathways. We have also demonstrated that distinct mesoderm subtypes, the lateral plate ($CD34^+KDR^+$) and paraxial ($CD34^-PDGFRα^+$) mesoderm, can be efficiently and rapidly derived as early as the third day of differentiation. The ability to generate various mesoderm derivatives may provide opportunities to establish model systems to study the underlying mechanisms regulating mesoderm specification in humans. More importantly, our study presents a unique approach in driving hESC differentiation toward mesoderm lineage cell types in a chemically directed fashion, which may be useful for future applications in regenerative medicine. Besides ESCs, the landmark discovery of induced PSCs (iPSCs) that are derived from human somatic cells through ectopic expression of transcription factors have also become a major development toward patient-specific cell therapy, drug discovery, and disease modeling in recent years [51,52]. Research is also increasingly focused on combining iPSCs with gene therapy for treatment of human diseases via gene targeting or gene augmentation therapy [53,54]. As such, our findings in this study may also be applicable for iPSC technology.

Acknowledgments

Author Disclosure Statement

References

1. Thomson J, J Itskovitz-Eldor, S Shapiro, M Waknitz, J Swiergiel, V Marshall and J Jones. (1998). Embryonic stem cell lines derived from human blastocysts. Science 282:1145–1147.
2. Murry C and G Keller. (2008). Differentiation of embryonic stem cells to clinically relevant populations: lessons from embryonic development. Cell 132:661–680.
3. Yang L, M Soonpaa, E Adler, T Roepke, S Kattman, M Kennedy, E Henckaerts, K Bonham, G Abbott, et al. (2008). Human cardiovascular progenitor cells develop from a KDR+ embryonic-stem-cell-derived population. Nature 453:524–528.
4. Park S, Y Jun Koh, J Jeon, Y Cho, M Jang, Y Kang, M Kim, C Choi, Y Sook Cho, et al. (2010). Efficient differentiation of human pluripotent stem cells into functional CD34+ progenitor cells by combined modulation of the MEK/ERK and BMP4 signaling pathways. Blood 116:5762–5772.
5. Levenberg S, J Zoldan, Y Basevitch and R Langer. (2006). Endothelial potential of human embryonic stem cells. Blood 110:806–814.
6. Wang C, X Tang, X Sun, Z Miao, Y Lv, Y Yang, H Zhang, P Zhang, Y Liu, et al. (2012). TGFβ inhibition enhances the generation of hematopoietic progenitors from human ES

cell-derived hemogenic endothelial cells using a stepwise strategy. Cell Res 22:194–207.

7. Matsumoto K, T Isagawa, T Nishimura, T Ogaeri, K Eto, S Miyazaki, J Miyazaki, H Aburatani, H Nakauchi and H Ema. (2009). Stepwise development of hematopoietic stem cells from embryonic stem cells. PLoS One 4:e4820.

8. Leeper N, A Hunter and J Cooke. (2010). Stem cell therapy for vascular regeneration: adult, embryonic, and induced pluripotent stem cells. Circulation 122:517–526.

9. Nir S, R David, M Zaruba, W Franz and J Itskovitz-Eldor. (2003). Human embryonic stem cells for cardiovascular repair. Cardiovasc Res 58:313–323.

10. Darabi R, K Gehlbach, R Bachoo, S Kamath, M Osawa, K Kamm, M Kyba and R Perlingeiro. (2008). Functional skeletal muscle regeneration from differentiating embryonic stem cells. Nat Med 14:134–143.

11. Iida M, T Heike, M Yoshimoto, S Baba, H Doi and T Nakahata. (2005). Identification of cardiac stem cells with FLK1, CD31, and VE-cadherin expression during embryonic stem cell differentiation. FASEB J 19:371–378.

12. Kataoka H, N Takakura, S Nishikawa, K Tsuchida, H Kodama, T Kunisada, W Risau, T Kita and S Nishikawa. (1997). Expressions of PDGF receptor alpha, c-Kit and Flk1 genes clustering in mouse chromosome 5 define distinct subsets of nascent mesodermal cells. Dev Growth Differ 39:729–740.

13. Sakurai H, T Era, L Jakt, M Okada, S Nakai, S Nishikawa and S Nishikawa. (2006). *In vitro* modeling of paraxial and lateral mesoderm differentiation reveals early reversibility. Stem Cells 24:575–586.

14. Tam P and R Behringer. (1997). Mouse gastrulation: the formation of a mammalian body plan. Mech Dev 68:3–25.

15. Kelly O, K Pinson and W Skarnes. (2004). The Wnt co-receptors Lrp5 and Lrp6 are essential for gastrulation in mice. Development 131:2803–2815.

16. Huelsken J, R Vogel, V Brinkmann, B Erdmann, C Birchmeier and W Birchmeier. (2000). Requirement for beta-catenin in anterior-posterior axis formation in mice. J Cell Biol 148:567–578.

17. van Amerongen R and A Berns. (2006). Knockout mouse models to study Wnt signal transduction. Trends Genet 22:678–689.

18. Liu P, M Wakamiya, M Shea, U Albrecht, R Behringer and A Bradley. (1999). Requirement for Wnt3 in vertebrate axis formation. Nat Genet 22:361–365.

19. Gadue P, T Huber, P Paddison and G Keller. (2006). Wnt and TGF-beta signaling are required for the induction of an *in vitro* model of primitive streak formation using embryonic stem cells. Proc Natl Acad Sci U S A 103:16806–16811.

20. Lindsley R, J Gill, M Kyba, T Murphy and K Murphy. (2006). Canonical Wnt signaling is required for development of embryonic stem cell-derived mesoderm. Development 133:3787–3796.

21. Lyashenko N, M Winter, D Migliorini, T Biechele, R Moon and C Hartmann. (2011). Differential requirement for the dual functions of β-catenin in embryonic stem cell self-renewal and germ layer formation. Nat Cell Biol 13:753–761.

22. Wray J, T Kalkan, S Gomez-Lopez, D Eckardt, A Cook, R Kemler and A Smith. (2011). Inhibition of glycogen synthase kinase-3 alleviates Tcf3 repression of the pluripotency network and increases embryonic stem cell resistance to differentiation. Nat Cell Biol 13:838–845.

23. Soncin F, L Mohamet, D Eckardt, S Ritson, A Eastham, N Bobola, A Russell, S Davies, R Kemler, C Merry and C Ward. (2009). Abrogation of E-cadherin-mediated cell-cell contact

in mouse embryonic stem cells results in reversible LIF-independent self-renewal. Stem Cells 27:2069–2080.

24. Ying Q, J Wray, J Nichols, L Batlle-Morera, B Doble, J Woodgett, P Cohen and A Smith. (2008). The ground state of embryonic stem cell self-renewal. Nature 453:519–523.

25. Sato N, L Meijer, L Skaltsounis, P Greengard and A Brivanlou. (2004). Maintenance of pluripotency in human and mouse embryonic stem cells through activation of Wnt signaling by a pharmacological GSK-3-specific inhibitor. Nat Med 10:55–63.

26. Ullmann U, C Gilles, M De Rycke, H Van de Velde, K Sermon and I Liebaers. (2008). GSK-3-specific inhibitor-supplemented hESC medium prevents the epithelial-mesenchymal transition process and the up-regulation of matrix metalloproteinases in hESCs cultured in feeder-free conditions. Mol Hum Reprod 14:169–179.

27. Davidson K, A Adams, J Goodson, C McDonald, J Potter, J Berndt, T Biechele, R Taylor and R Moon. (2012). Wnt/β-catenin signaling promotes differentiation, not self-renewal, of human embryonic stem cells and is repressed by Oct4. Proc Natl Acad Sci U S A 109:4485–4490.

28. Bone H, A Nelson, C Goldring, D Tosh and M Welham. (2011). A novel chemically directed route for the generation of definitive endoderm from human embryonic stem cells based on inhibition of GSK-3. J Cell Sci 124:1992–2000.

29. Nakanishi M, A Kurisaki, Y Hayashi, M Warashina, S Ishiura, M Kusuda-Furue and M Asashima. (2009). Directed induction of anterior and posterior primitive streak by Wnt from embryonic stem cells cultured in a chemically defined serum-free medium. FASEB J 23:114–122.

30. Vo E, D Hanjaya-Putra, Y Zha, S Kusuma and S Gerecht. (2010). Smooth-muscle-like cells derived from human embryonic stem cells support and augment cord-like structures *in vitro*. Stem Cell Rev 6:237–247.

31. Ng E, L Azzola, K Sourris, L Robb, E Stanley and A Elefanty. (2005). The primitive streak gene Mixl1 is required for efficient haematopoiesis and BMP4-induced ventral mesoderm patterning in differentiating ES cells. Development 132:873–884.

32. Wilkinson D, S Bhatt and B Herrmann. (1990). Expression pattern of the mouse T gene and its role in mesoderm formation. Nature 343:657–659.

33. Burtscher I and H Lickert. (2009). Foxa2 regulates polarity and epithelialization in the endoderm germ layer of the mouse embryo. Development 136:1029–1038.

34. Tada S, T Era, C Furusawa, H Sakurai, S Nishikawa, M Kinoshita, K Nakao, T Chiba and S Nishikawa. (2005). Characterization of mesendoderm: a diverging point of the definitive endoderm and mesoderm in embryonic stem cell differentiation culture. Development 132:4363–4374.

35. Pick M, L Azzola, A Mossman, E Stanley and A Elefanty. (2007). Differentiation of human embryonic stem cells in serum-free medium reveals distinct roles for bone morphogenetic protein 4, vascular endothelial growth factor, stem cell factor, and fibroblast growth factor 2 in hematopoiesis. Stem Cells 25:2206–2214.

36. Rufaihah A, N Huang, S Jamé, J Lee, H Nguyen, B Byers, A De, J Okogbaa, M Rollins, et al. (2011). Endothelial cells derived from human iPSCS increase capillary density and improve perfusion in a mouse model of peripheral arterial disease. Arterioscler Thromb Vasc Biol 31:e72–79.

37. Xu R, X Chen, D Li, R Li, G Addicks, C Glennon, T Zwaka and J Thomson. (2002). BMP4 initiates human embryonic stem cell differentiation to trophoblast. Nat Biotechnol 20:1261–1264.

38. Pera M, J Andrade, S Houssami, B Reubinoff, A Trounson, E Stanley, D Ward-van Oostwaard and C Mummery. (2004). Regulation of human embryonic stem cell differentiation by BMP-2 and its antagonist noggin. J Cell Sci 117:1269–1280.

39. Lee T, J Jang, S Kang, M Jin, H Shin, D Kim and B Kim. (2013). Enhancement of osteogenic and chondrogenic differentiation of human embryonic stem cells by mesodermal lineage induction with BMP-4 and FGF2 treatment. Biochem Biophys Res Commun 430:793–797.

40. Zhang P, J Li, Z Tan, C Wang, T Liu, L Chen, J Yong, W Jiang, X Sun, et al. (2008). Short-term BMP-4 treatment initiates mesoderm induction in human embryonic stem cells. Blood 111:1933–1941.

41. Yamashita J, H Itoh, M Hirashima, M Ogawa, S Nishikawa, T Yurugi, M Naito, K Nakao and S Nishikawa. (2000). Flk1-positive cells derived from embryonic stem cells serve as vascular progenitors. Nature 408:92–96.

42. Evseenko D, Y Zhu, K Schenke-Layland, J Kuo, B Latour, S Ge, J Scholes, G Dravid, X Li, W MacLellan and G Crooks. (2010). Mapping the first stages of mesoderm commitment during differentiation of human embryonic stem cells. Proc Natl Acad Sci U S A 107:13742–13747.

43. MacDonald B, K Tamai and X He. (2005). Wnt/β-catenin signaling: components, mechanisms, and diseases. Dev Cell 17:9–26.

44. Kemler R, A Hierholzer, B Kanzler, S Kuppig, K Hansen, M Taketo, W de Vries, B Knowles and D Solter. (2004). Stabilization of beta-catenin in the mouse zygote leads to premature epithelial-mesenchymal transition in the epiblast. Development 131:5817–5824.

45. Dravid G, Z Ye, H Hammond, G Chen, A Pyle, P Donovan, X Yu and L Cheng. (2005). Defining the role of Wnt/beta-catenin signaling in the survival, proliferation, and self-renewal of human embryonic stem cells. Stem Cells 23:1489–1501.

46. Cai L, Z Ye, B Zhou, P Mali, C Zhou and L Cheng. (2007). Promoting human embryonic stem cell renewal or differentiation by modulating Wnt signal and culture conditions. Cell Res 17:62–72.

47. Ding V, L Ling, S Natarajan, M Yap, S Cool and A Choo. (2010). FGF-2 modulates Wnt signaling in undifferentiated hESC and iPS cells through activated PI3-K/GSK3beta signaling. J Cell Physiol 225:417–428.

48. Drukker M, C Tang, R Ardehali, Y Rinkevich, J Seita, A Lee, A Mosley, I Weissman and Y Soen. (2012). Isolation of primitive endoderm, mesoderm, vascular endothelial and trophoblast progenitors from human pluripotent stem cells. Nat Biotechnol 30:531–542.

49. Greber B, H Lehrach and J Adjaye. (2008). Control of early fate decisions in human ES cells by distinct states of TGFbeta pathway activity. Stem Cells Dev 17:1065–1077.

50. McLean A, K D'Amour, K Jones, M Krishnamoorthy, M Kulik, D Reynolds, A Sheppard, H Liu, Y Xu, E Baetge and S Dalton. (2007). Activin A efficiently specifies definitive endoderm from human embryonic stem cells only when phosphatidylinositol 3-kinase signaling is suppressed. Stem Cells 25:29–38.

51. Nelson T, A Martinez-Fernandez, S Yamada, C Perez-Terzic, Y Ikeda and A Terzic. (2009). Repair of acute myocardial infarction by human stemness factors induced pluripotent stem cells. Circulation 120:408–416.

52. Rufaihah A, N Huang, J Kim, J Herold, K Volz, T Park, J Lee, E Zambidis, R Reijo-Pera and J Cooke. (2013). Human induced pluripotent stem cell-derived endothelial cells exhibit functional heterogeneity. Am J Transl Res 5:21–35.

53. Sebastiano V, M Maeder, J Angstman, B Haddad, C Khayter, D Yeo, M Goodwin, J Hawkins, C Ramirez, et al. (2011). *In situ* genetic correction of the sickle cell anemia mutation in human induced pluripotent stem cells using engineered zinc finger nucleases. Stem Cells 29:1717–1726.

54. Raya A, et al. (2009). Disease-corrected haematopoietic progenitors from Fanconi anaemia induced pluripotent stem cells. Nature 460:53–59.

Address correspondence to:
Dr. Tong Cao
Oral Sciences
Faculty of Dentistry
National University of Singapore
11 Lower Kent Ridge Road
Singapore 119083
Singapore

E-mail: tong_cao@nuhs.edu.sg